論文 ・著書情報
Article ・Book Information

Title	Hydrogen anion and subgap states in amorphous In・Ga・Zn・O thin films for TFT applications
Authors	Joonho Bang・Satoru Matsuishi・Hideo Hosono
Citation	APPLIED PHYSICS LETTERS・Vol・110・No・23・ 232105
Pub・date	2017・6
DOI	http・・dx・doi・org・10・1063・1・4985627
Note	This article may be downloaded for personal use only・Any other use requires prior permission of the author and AIP Publishing・

Hydrogen anion and subgap states in amorphous In–Ga–Zn–O thin films for TFT applications

Joonho Bang, Satoru Matsuishi, and Hideo Hosono

Citation: Appl. Phys. Lett. **110**, 232105 (2017); doi: 10.1063/1.4985627
View online: http://dx.doi.org/10.1063/1.4985627
View Table of Contents: http://aip.scitation.org/toc/apl/110/23
Published by the American Institute of Physics

Hydrogen anion and subgap states in amorphous In–Ga–Zn–O thin films for TFT applications

Joonho Bang,[1] Satoru Matsuishi,[1] and Hideo Hosono[1,2,a)]
[1]*Materials Research Center for Element Strategy, Tokyo Institute of Technology, Yokohama 226-8503, Japan*
[2]*Materials and Structures Laboratory, Tokyo Institute of Technology, Yokohama 226-8503, Japan*

(Received 14 February 2017; accepted 31 May 2017; published online 8 June 2017)

Hydrogen is an impurity species having an important role in the physical properties of semiconductors. Despite numerous studies, the role of hydrogen in oxide semiconductors remains an unsolved puzzle. This situation arises from insufficient information about the chemical state of the impurity hydrogen. Here, we report direct evidence for anionic hydrogens bonding to metal cations in amorphous In–Ga–Zn–O (a-IGZO) thin films for thin-film transistors (TFT) applications and discuss how the hydrogen impurities affect the electronic structure of a-IGZO. Infrared absorption spectra of self-standing a-IGZO thin films prepared by sputtering reveal the presence of hydrogen anions as a main hydrogen species (concentration is $\sim 10^{20}\,cm^{-3}$) along with the hydrogens in the form of the hydroxyl groups ($\sim 10^{20}\,cm^{-3}$). Density functional theory calculations show that bonds between these hydride ions with metal centers give rise to subgap states above the top of the valence band, implying a crucial role of anionic hydrogen in the negative bias illumination stress instability commonly observed in a-IGZO TFTs. *Published by AIP Publishing.*
[http://dx.doi.org/10.1063/1.4985627]

Despite the long history of research on oxide semiconductors, the origins of several physical properties, such as subgap levels and photo-induced phenomena, are still under debate. Hydrogen, the most common impurity in oxides, has received attention as a key to understanding these long-disputed questions. Recent theoretical and experimental studies suggest that representative oxide semiconductors contain a significant number of hydrogen species and that their physical properties may be related to this presence of hydrogen.[1–4] The vital role of impurity hydrogen stimulates us to develop new ideas to understand physical phenomena that are difficult to explain with the traditional oxygen vacancy model. For example, recent studies on ZnO show that hydrogen may be the primary cause of n-type conductivity,[1,2] and this result is far beyond the traditional carrier generation mechanism: one oxygen vacancy generates two electrons. Therefore, the elucidation of the role of hydrogen in the oxide semiconductors is crucial for understanding the physics of semiconductors and may be a stepping-stone toward the next generation of semiconductor technology.

Oxide thin-film transistors (TFTs), especially amorphous In–Ga–Zn–O (a-IGZO)[5] TFT, are attracting industrial interest for the backplanes of high resolution liquid crystal displays and large-sized organic light-emitting diode displays. This is due to their high mobilities (higher by an order of magnitude than that of a-Si:H) and the ease of producing such large-sized thin films with the conventional sputtering technique. The largest technical issue remaining for applications is the negative bias illumination stress (NBIS) instability, i.e., a negative shift of the threshold voltage occurs when a negative gate bias is applied under light-illumination, which unfortunately corresponds to the major operation state of the displays. NBIS instability is commonly observed in oxide TFTs such as c-ZnO[6] and a-In–Zn–O,[7] Zn–Sn–O,[8] In–Ga–Zn–O,[9] In–Sn–Zn–O,[10] and Hf–In–Zn–O,[11] regardless of whether the materials are crystalline or amorphous. For a-IGZO TFTs, NBIS instability is observed under light with photon energies as low as 2.3 eV, which is lower than the band gap energy of ~3 eV.[9] This result strongly suggests that the NBIS instability is closely related to the subgap states.[12] Absorption tails are apparent in the optical spectra at these low photon energies, suggesting the presence of subgap states. Indeed, hard X-ray photoemission measurements (a bulk sensitive probe) reveal that occupied subgap levels are present near the valence band maximum (VBM) with a density of states (DOS) of $\sim 10^{20}\,cm^{-3}$.[13] Therefore, the primary origin of the subgap absorption can be interpreted in terms of electronic transitions from these tail states to the conduction band. From these results, a plausible model for NBIS instability can be proposed: the photoexcitation of the subgap states promotes an electron at the conduction band, leaving a positive hole in the subgap states. Under negative bias, the resulting hole then drifts to the interface between the gate insulator and a-IGZO, giving rise to a negative shift of the TFT threshold.[9] To suppress the NBIS instability in a-IGZO TFTs, it is thus crucial to clarify the entity responsible for the subgap states. One clue is the fact that a-IGZO thin films contain hydrogen impurities at the level of $\sim 10^{20}\,cm^{-3}$, even though no intentional hydrogen source is used during the fabrication processes.[14]

Hydrogen is the simplest element in the periodic table, but has a rich chemical variety. The valence state can vary from +1 to −1, resulting in an exceptionally enormous range of the ionic size; the ionic radii of H^+, H^0, and H^- are almost zero, 63, and 130 pm, respectively, and the ionic radius of H^- varies over several tens of percent depending on the local environment.[15] Clarifying the chemical state of hydrogen is therefore critical for the elucidation of the role of hydrogen

a)E-mail: hosono@msl.titech.ac.jp

impurities in oxide semiconductors. Impurity hydrogen is thought to exist in amorphous oxide semiconductors primarily in hydroxyl groups (OH^-), where the H atoms would have a partial positive charge. In this study, we report direct evidence for the existence of hydride ions (H^-) bound to metal cations in a-IGZO thin films, using a combination of infrared absorption spectroscopy and thermal desorption spectroscopy (TDS), and discuss the relationship between the H^- ions and the subgap states.

Infrared absorption spectroscopy is a powerful technique for investigating the bonding state of the constituent atoms or ions of amorphous materials. However, hydrogen is a challenge in an amorphous thin-film due to its small concentration (<1 at. %). In addition, the lattice and impurity absorption signals originating from the substrate complicate the collection of intrinsic vibrational modes associated with impurity hydrogen species. To eliminate any absorption originating from the substrate, we prepared self-standing films: a-IGZO films were deposited on single crystalline NaCl substrates and the resulting thin films released by dissolving the substrate in water. To obtain the absorption spectra with S/N ratios large enough to analyze, the a-IGZO films were grown ~2 μm thickness. The thin films were deposited at room temperature by conventional radio-frequency magnetron sputtering using a dense ceramic $InGaZnO_4$ target. Before deposition, the chamber was pumped by a turbo-molecular pump until a base pressure of 10^{-4} Pa was achieved. The total pressure during deposition was maintained at 0.55 Pa by using an $O_2 + Ar$ gas mixture [$O_2/(O_2 + Ar) = 2\%$]. These deposition conditions and methods are essentially the same as those used in the fabrication of a-IGZO TFTs. After deposition, some films were annealed at 300 to 800 °C in an oxygen gas flow for 1 h. Infrared transmittance and reflectance spectra were collected with the Fourier transformation spectroscopy method (VERTEX 70v, Bruker) under vacuum at room temperature. To evaluate the amount of hydrogen incorporated in the thin films, the measurements of TDS were carried out in a vacuum chamber with a background pressure of 1.5×10^{-7} Pa, from room temperature to 1200 °C at a heating rate of 60 °C min^{-1}.

First-principles density functional theory (DFT) calculations were performed using the generalized gradient approximation with the Perdew – Burke – Ernzerhof functional[16,17] and the projector augmented plane-wave method implemented in the Vienna *ab initio* simulation program code.[18] On-site Coulomb interaction values of 7, 8, and 8 eV were used for the In 4d, Ga 3d, and Zn 3d orbitals, respectively.[19] A a-IGZO model[20] relaxed with molecular dynamics was used as a starting point for the calculation, and the plane-wave basis set cut-off energy was set to 800 eV. A k-point mesh of $3 \times 3 \times 3$ was used for ionic relaxation, and a mesh of $5 \times 5 \times 5$ was used to calculate the DOS and charge density distribution. Structural relaxations were performed until the Hellmann–Feynman forces were less than 10^{-5} eV $Å^{-1}$. The Born effective charge tensors and force constant matrices were then constructed by density functional perturbation theory and the finite differences method to calculate the spectra of infrared-active modes for H-free a-IGZO and hydrogen-incorporated a-IGZO, respectively.

Figure 1(a) shows the infrared transmittance and reflectance spectra of self-standing a-IGZO thin film at room temperature. The absorption coefficients α [Fig. 1(b)] were estimated from the equation $\alpha = -\ln[T/(1-R)]/d$, where T and R are the transmittance and reflectance shown in Fig. 1(a), and d is the film thickness. The absorption below 1000 cm^{-1} is reproduced well by calculated infrared spectrum of a-IGZO (orange lines); these absorptions are attributed to the vibrational modes of the M (In, Ga, and Zn)–O bonds constituting the lattice. Four additional bands appear in the spectrum: three sharp bands at 1039, 1389, and 1524, as well as a broad band at ~3000 cm^{-1} [Fig. 1(c)]. The last of these can be assigned to the stretching mode of hydroxyl groups (OH^-) involved in hydrogen bonding.[14] The frequencies for two absorption bands at 1389 and 1524 cm^{-1} are attributed to the M–H bonds based on their close match in frequency to those of the gaseous hydride molecules InH (1475 cm^{-1}), GaH (1604 cm^{-1}), and ZnH (1616 cm^{-1}).[21]

To investigate the detailed chemical states and vibrational modes of hydrogen in a-IGZO, DFT calculations were performed on hydrogen-incorporated models. Several models were evaluated by comparison with the experimental data; it was found that M–H bonds could be stabilized when hydrogens are positioned at oxygen vacancy sites. Red lines in Fig. 1(c) show the calculated infrared absorption spectrum that best fits the experimental one, while the vibrational mode for each absorption band is shown in Figs. 2(c)–2(e).

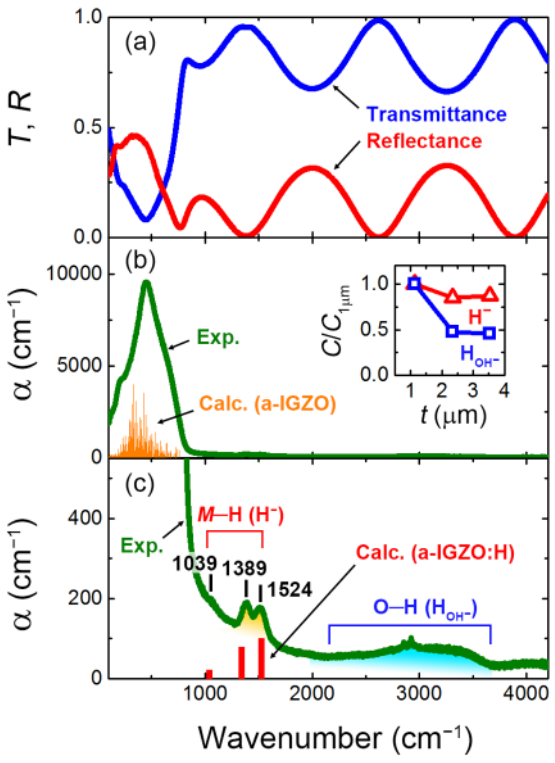

FIG. 1. Experimental and calculated infrared spectra of a-IGZO thin films. (a) Measured infrared transmittance (T) and reflectance (R) spectra of a self-standing a-IGZO thin film. (b) and (c) Absorption coefficients (α) calculated from the observed transmittance and reflectance spectra. Orange and red lines indicate the calculated infrared spectra of H-free a-IGZO and hydrogen-containing a-IGZO (a-IGZO:H). The inset shows the thickness (t) dependence of the concentrations (C) of H_{OH^-} and H^- estimated from infrared spectra. The concentration is normalized by the value for a 1 μm thick sample.

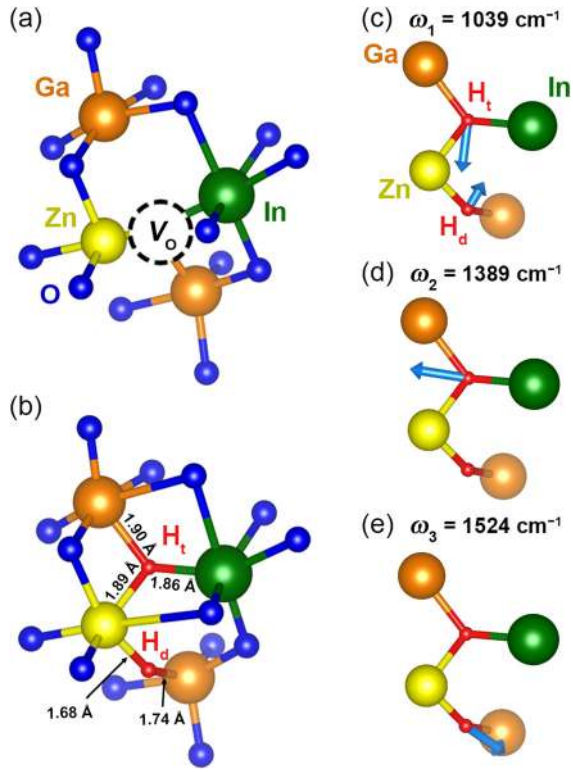

FIG. 2. Local structure of hydrogen containing a-IGZO. (a) The oxygen vacancy model before the structural relaxation as an initial structure for hydrogen containing a-IGZO. (b) The local structure of the hydrogen-incorporated a-IGZO. H_t and H_d indicate the triply and doubly coordinated hydrogen atoms, respectively. (c)–(e) Calculated vibrational modes corresponding to peaks indicated in Fig. 1(c). Blue arrows indicate the directions of atomic motion.

In this model, a neutral oxygen vacancy coordinated by three cations [Fig. 2(a)] reacts with a hydrogen molecule. An H_2 molecule splits into two H^- ions by the reaction with 2 electrons at the oxygen vacancy, a process analogous to the oxidative addition reaction of molecular transition metal chemistry. Figure 2(b) shows the local structure around the H^- ions after relaxation. One hydrogen (H_t) is coordinated by three metal cations (In, Ga, and Zn) and another hydrogen (H_d) is doubly coordinated by two metal cations (Ga and Zn). As shown in Figs. 2(d) and 2(e), the displacement vectors (blue arrows) for the vibrational modes responsible for the bands at 1389 and 1524 cm^{-1} are almost parallel to the In–H and Zn–H bonds. The frequencies are slightly red-shifted by 86 and 92 cm^{-1} compared to those of the corresponding hydride molecules.[21] This shift is understandable considering that the *M*–H stretching modes in hydride molecules are isolated, while those in a-IGZO are coupled with its nearby ions constituting the lattice which may suppress the *M*–H stretching modes. Thus, the calculation substantiates the assignment of the observed infrared bands to *M*–H bonds.

The inset of Fig. 1 shows the thickness dependence of the concentrations for the O–H bond (H_{OH^-}) and *M*–H bond (H^-), as judged from the infrared spectra. There is no significant change in the concentrations of H_{OH^-} and H^- when the film thickness is sufficiently thick (above 2 μm), while the hydrogen concentrations increase with decreasing of thickness below 2 μm. This increase in the hydrogen content suggests that there is a higher concentration of defects accommodating O–H and *M*–H bonds near the film-substrate interface and/or the surface region. A similar trend was also observed in the depth vs. concentration profile for hydrogen determined by secondary ion mass spectrometry.[14]

Figure 3(a) shows how absorption spectra change with the post-annealing temperature. The absorption peaks responsible for the IGZO lattice structure (below 1000 cm^{-1}) became sharper above 600 °C. This change is attributed to the crystallization of a-IGZO.[22] As crystallization proceeds, the O–H absorption peak gradually decreases and finally disappears, while the absorption peaks for the *M*–H bonds remain after crystallization is completed. The variation in the concentration of O–H (H_{OH^-}) and *M*–H (H^-) bonds with annealing temperature is plotted in Fig. 3(c). The

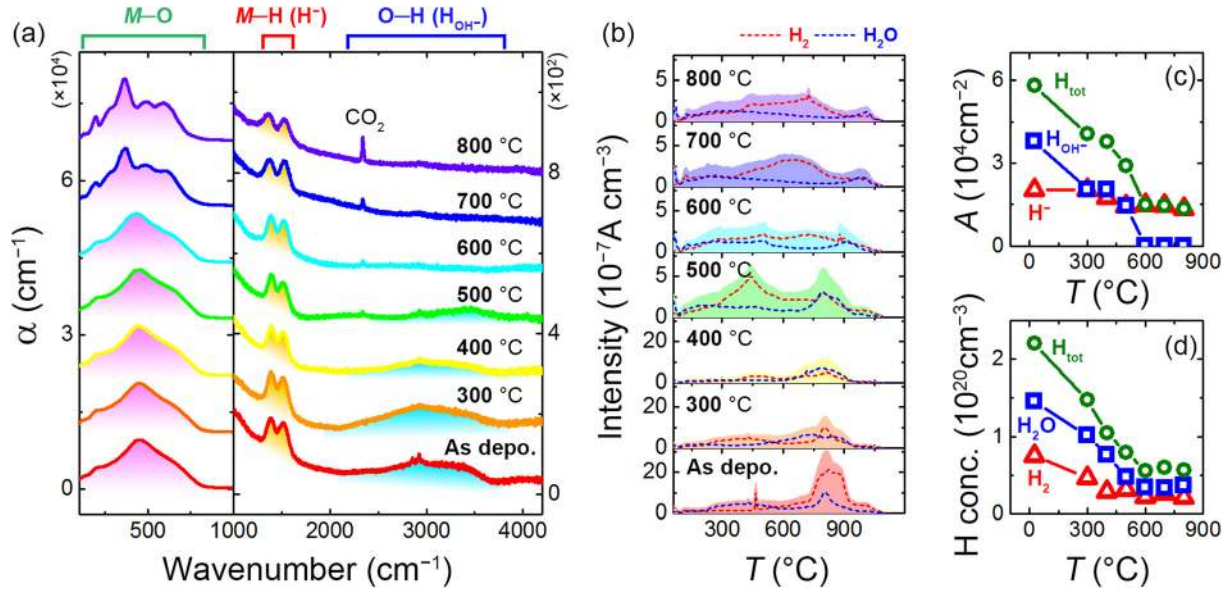

FIG. 3. Thermal stability of H_{OH^-} and H^-. (a) Infrared and (b) TDS spectra of self-standing IGZO thin films post annealed under flowing oxygen gas. (c) Integrated peak areas for *M*–H (H^-) and O–H (H_{OH^-}) vibrational modes. (d) Hydrogen concentrations desorbed as H_2 and H_2O upon heating. Data were obtained from TDS spectra.

concentration of H_{OH^-} gradually decreases as the temperature is raised and disappears around 600 °C. In contrast, the concentration of H^- ions decreases by only ~30% up to the onset of crystallization (600 °C), and ~70% of the H^- remains after the crystallization is completed. We infer that the interstitial hydrogens incorporated as OH^- are almost eliminated during the crystallization process, but the major portion of H^- is retained even after crystallization, indicating that the H^- ions substituting for the oxygen vacancy site are thermally stable.

Figures 3(b) and 3(d) show the variation in the TDS profile and the amount of desorbed hydrogen as a function of post annealing temperature for the self-standing a-IGZO thin films. The total hydrogen concentration calculated by adding the amounts detected as H_2 and H_2O molecules shows the same trend as the infrared data. The concentration of H^- (C_{H^-}) in the as-deposited sample can be estimated from $C_{H^-} = \beta \times A_{H^-}$, where β is a constant depending on the types of bonding, and A_{H^-} is the integrated peak area of *M*–H modes in the infrared spectrum. The coefficient $\beta = 3.75 \times 10^{15}\,cm^{-1}$ can be obtained by using the total hydrogen concentration obtained from the TDS data and the A_{H^-} value from the infrared spectrum of the sample post annealed at 600 °C, where all H atoms occur as H^- described above. Once this relationship is established, the amounts of H^- and H_{OH^-} in the as-deposited a-IGZO sample can be estimated as $\sim 7.6 \times 10^{19}\,cm^{-3}$ (~0.1 at. %) and $\sim 1.5 \times 10^{20}\,cm^{-3}$ (~0.2 at. %), respectively.

The computational results presented earlier allow us to derive a simple bonding scheme connecting the hydrogen impurities and subgap states in a-IGZO. Figure 4 shows the total and partial DOS calculated on the structural model for H-incorporated in a-IGZO whose calculated infrared spectrum best matches the observed one [Fig. 1(c)]. The insets of Figs. 4(a) and 4(b) show the isosurfaces (0.01 electrons/Å) of the charge density distributions for the subgap DOS features with and without H, respectively. For the oxygen vacancy model [Fig. 4(b)], the subgap DOS is located at ~1.1 eV above the VBM and the electrons occupying these states are distributed around the oxygen vacancy. When including the hydrogen [Fig. 4(a)], the subgap DOS shifts down to ~0.4 eV above the VBM and the H 1s orbital is the dominant contributor to the subgap states. When we recall the computational conclusion of Fig. 2(b), where a neutral oxygen vacancy is stabilized by the incorporation of H as H^-, this result strongly suggests that the subgap states near the VBM originate from *M*–H bonding orbitals with high H 1s character. This picture is summarized in Fig. 4(c) with a schematic diagram of the electronic structure of a-IGZO including H^-.

Let us now discuss how such H^- impurities can be incorporated and stabilized at the oxygen vacancy sites in the preparation of a-IGZO thin films. It is well known that in ionic oxide crystals, such as alkaline earth oxides, H^- ion substitutes for oxygen ion sites when an oxide crystal with a cation-rich stoichiometry is heated in a H_2-bearing atmosphere.[23,24] This may be understood by the fact that an oxygen vacancy is stabilized by substitution of H^- ion as was recently confirmed by experiment and calculations on iron-based superconductors $LnFeAsO_{1-x}H_x$ (*Ln* denotes

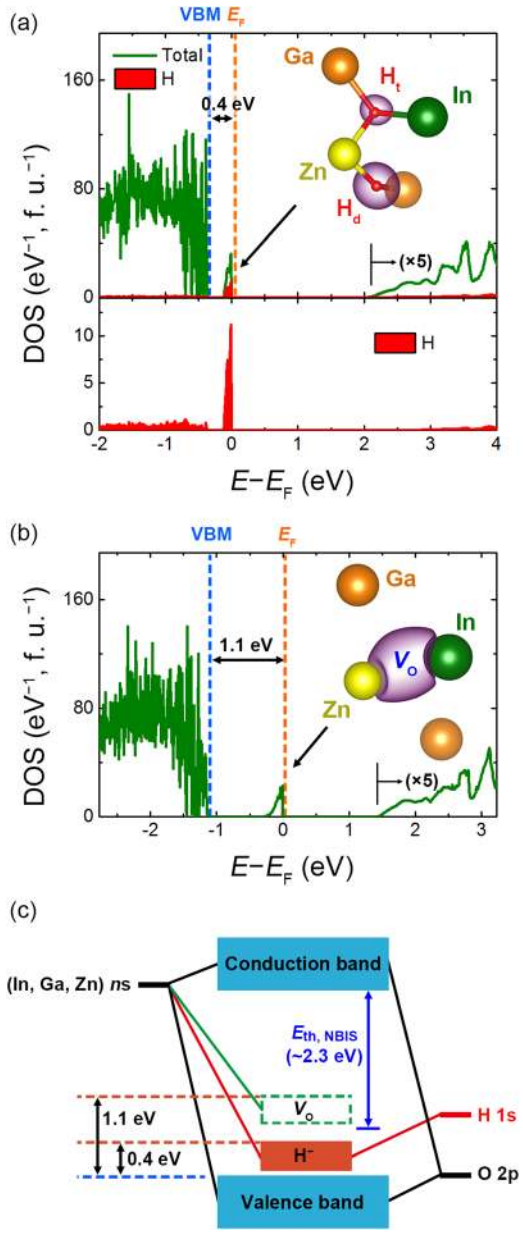

FIG. 4. Subgap states of hydrogen-incorporated a-IGZO. (a) Total and partial DOS of hydrogen-incorporated a-IGZO. (b) Total DOS in oxygen vacancy model [see Fig. 2(a)]. Insets of (a) and (b) show the isosurfaces (0.01 electrons/Å) of charge density distributions for each subgap DOS feature. (c) Schematic diagram of the subgap states in a-IGZO thin films. Blue arrow indicates the threshold photon energy for NBIS phenomenon ($E_{th, NBIS}$).

lanthanide).[25] In the present case, amorphous oxide semiconductor thin films were deposited by a conventional sputtering method in a vacuum chamber that was evacuated with a turbo-molecular pump. Since the main residual gases in such a deposition chamber are H_2 and H_2O, these species are likely present during the growth of the film. Also, during the thin film deposition process, the oxygen vacancy formation is made possible because sputtering process is composed of formation of transient high temperature states by atomic collisions between ionized sputtering gas (Ar^+) and the target material (crystalline IGZO) and the subsequent rapid quenching upon deposition on the substrate (NaCl single crystal). As a high concentration of oxygen vacancies is generated transiently, they are able to react with the H_2 and/or

H_2O in the deposition chamber. It is thus understandable that the as-deposited a-IGZO thin films contain high concentrations of *M*–H and O–H bonds.

These results have implications for the origins of the NBIS instability of oxide TFTs in general. There is a consensus that NBIS instability occurs due to the accumulation of subgap positive charge under bias to the gate insulator, which is induced by photoexcitation of subgap states near the VBM. The issue has been identifying the major entity responsible for the subgap states, with proposed candidates including oxygen vacancies, excess oxygen-type defects, low valence states metal, and H-related species. However, no direct experimental evidence has thus far been reported. The present study combining spectroscopic and computational results indicates that the subgap states arise from *M*–H bonds in a-IGZO, which form as H^- ions are stabilized at the oxygen vacancy sites. The photoexcitation of H^- is found in several oxides such as MgO[26,27] and C12A7:H^-[15,28,29]. In these compounds, the chemical state of hydrogen is quite similar to that in a-IGZO thin films; both OH^- species and H^- occupying oxygen sites coexist. It is noteworthy that the formation of F_s^+(H) color centers in MgO and the photo-activated conduction of C12A7:H^- are induced by the photodissociation of H^- ($H^- + h\nu \rightarrow H^0 + e^-$). Because neutral H^0 is rather mobile, it can migrate and recombine with electrons ($H^0 + e^- \rightarrow H^-$) or react with O^{2-} to form OH^- ($H^0 + O^{2-} \rightarrow OH^- + e^-$). Further studies are in progress aimed at elucidating the mechanism of the NBIS instability and ultimately suppressing it.

We acknowledge Dr. Toshio Kamiya, Dr. Hideya Kumomi, Dr. Hiroshi Mizoguchi, Dr. Daniel C. Fredrickson, Dr. Taku Hanna, Dr. Yoshinori Muraba, and Dr. Keisuke Ide for valuable discussions. This study was supported by MEXT, Element Strategy Initiative to form a research core.

[1]C. G. Van De Walle, Phys. Rev. Lett. **85**, 1012 (2000).
[2]D. M. Hofmann, A. Hofstaetter, F. Leiter, H. Zhou, F. Henecker, B. K. Meyer, S. B. Orlinskii, J. Schmidt, and P. G. Baranov, Phys. Rev. Lett. **88**, 45504 (2002).
[3]C. G. Van de Walle and J. Neugebauer, Nature **423**, 626 (2003).
[4]M. H. Du and K. Biswas, Phys. Rev. Lett. **106**, 115502 (2011).
[5]K. Nomura, H. Ohta, A. Takagi, T. Kamiya, M. Hirano, and H. Hosono, Nature **432**, 488 (2004).
[6]P. Barquinha, E. Fortunato, A. Gonçalves, A. Pimentel, A. Marques, L. Pereira, and R. Martins, Superlattices Microstruct. **39**, 319 (2006).
[7]P. Barquinha, A. Pimentel, A. Marques, L. Pereira, R. Martins, and E. Fortunato, J. Non-Cryst. Solids **352**, 1756 (2006).
[8]P. Görrn, P. Hölzer, T. Riedl, W. Kowalsky, J. Wang, T. Weimann, P. Hinze, and S. Kipp, Appl. Phys. Lett. **90**, 63502 (2007).
[9]K. Nomura, T. Kamiya, and H. Hosono, J. Soc. Inf. Disp. **18**, 789 (2010), available at http://onlinelibrary.wiley.com/doi/10.1889/JSID18.10.789/abstract.
[10]J. Jang, D. G. Kim, D. M. Kim, S. J. Choi, J. H. Lim, J. H. Lee, Y. S. Kim, B. Du Ahn, and D. H. Kim, Appl. Phys. Lett. **105**, 152108 (2014).
[11]J. S. Park, T. S. Kim, K. S. Son, J. S. Jung, K. Lee, J. Kwon, B. Koo, and S. Lee, IEEE Electron Device Lett. **31**, 440 (2010).
[12]H. H. Hsieh, T. Kamiya, K. Nomura, H. Hosono, and C. C. Wu, Appl. Phys. Lett. **92**, 133503 (2008).
[13]K. Nomura, T. Kamiya, H. Yanagi, E. Ikenaga, K. Yang, K. Kobayashi, M. Hirano, and H. Hosono, Appl. Phys. Lett. **92**, 202117 (2008).
[14]K. Nomura, T. Kamiya, and H. Hosono, ECS J. Solid State Sci. Technol. **2**, P5 (2013).
[15]K. Hayashi, P. V. Sushko, Y. Hashimoto, A. L. Shluger, and H. Hosono, Nat. Commun. **5**, 3515 (2014).
[16]J. P. Perdew, K. Burke, and M. Ernzerhof, Phys. Rev. Lett. **77**, 3865 (1996).
[17]J. P. Perdew, K. Burke, and M. Ernzerhof, Phys. Rev. Lett. **78**, 1396 (1997).
[18]G. Kresse and J. Furthmüller, Phys. Rev. B **54**, 11169 (1996).
[19]B. Ryu, H.-K. Noh, E.-A. Choi, and K. J. Chang, Appl. Phys. Lett. **97**, 22108 (2010).
[20]K. Nomura, T. Kamiya, H. Ohta, T. Uruga, M. Hirano, and H. Hosono, Phys. Rev. B **75**, 35212 (2007).
[21]S. Aldridge and A. J. Downs, Chem. Rev. **101**, 3305 (2001).
[22]K. Ide, K. Nomura, H. Hiramatsu, T. Kamiya, and H. Hosono, J. Appl. Phys. **111**, 073513 (2012).
[23]Y. Chen, R. Gonzalez, O. E. Schow, and G. P. Summers, Phys. Rev. B **27**, 1276 (1983).
[24]G. Pacchioni and A. Maria Ferrari, Catal. Today **50**, 533 (1999).
[25]Y. Muraba, S. Iimura, S. Matsuishi, and H. Hosono, Inorg. Chem. **54**, 11567 (2015).
[26]E. Giamello, M. C. Paganini, D. M. Murphy, A. M. Ferrari, and G. Pacchioni, J. Phys. Chem. B **101**, 971 (1997).
[27]D. Ricci, C. Di Valentin, G. Pacchioni, P. V. Sushko, A. L. Shluger, and E. Giamello, J. Am. Chem. Soc. **125**, 738 (2003).
[28]S. Matsuishi, K. Hayashi, M. Hirano, and H. Hosono, J. Am. Chem. Soc. **127**, 12454 (2005).
[29]K. Hayashi, P. V. Sushko, A. L. Shluger, M. Hirano, and H. Hosono, J. Phys. Chem. B **109**, 23836 (2005).